Physica B 521 (2017) 13–16

Contents lists available at ScienceDirect

Physica B

journal homepage: www.elsevier.com/locate/physb

Structural stability and phase transition of Bi_2Te_3 under high pressure and low temperature

J.L. Zhang[a,b,*], S.J. Zhang[b], J.L. Zhu[b], Q.Q. Liu[b], X.C. Wang[b], C.Q. Jin[b,**], J.C. Yu[a]

[a] Faculty of Electrical Engineering and Computer Science, Ningbo University, Ningbo 315211, China
[b] Institute of Physics, Chinese Academy of Sciences, Beijing 100190, China

ARTICLE INFO

Keywords:
High pressure
Low temperature
Phase transition
X-ray diffraction
Topological superconductivity

ABSTRACT

Structural stability and phase transition of topological insulator Bi_2Te_3 were studied via angle-dispersive synchrotron radiation X-ray diffraction under high pressure and low temperature condition. The results manifest that the *R*-3*m* phase (phase I) is stable at 8 K over the pressure range up to 10 GPa and phase transition occurs between 8 K and 45 K at 8 GPa. According to the Birch-Murnaghan equation of state, the bulk modulus at ambient pressure B_0 was estimated to be 45 ± 3 GPa with the assumption of $B_0' = 4$. The structural robustness of phase I at 8 K suggests that the superconductivity below 10 GPa is related to phase I. Topological properties of superconducting Bi_2Te_3 phase under pressure were discussed.

1. Introductions

The discovery of topological insulators [1–6] unveiled a new realm of topological quantum matters. Their intriguing physical phenomena with promising application potentials greatly attracted the attention of physicists and materials scientists [7–10]. Topological insulators have gaped bulk states like ordinary insulators coexisting with symmetry-protected robust gapless surface states on their edges or interfaces [11,12]. Majorana fermions, which obey non-Abelian statistics, were expected to exist at the interfaces between topological insulators and superconductors [7]. Majorana fermions are also thought to survive in topological superconductors which have symmetry-protected gapless surface states coexisting with superconducting states in bulk [13].

Bi_2Te_3 is one of the earliest experimentally confirmed topological insulators [6]. Crystal structures at room temperature and high pressure have been studied by several research groups [14–20]. At room temperature and ambient pressure, Bi_2Te_3 has a rhombohedral structure with space group *R*-3*m* (Phase I). With increasing pressure, R-3m structure transforms to *C*2/*m* (Phase II) at 8 GPa, to *C*2/*c* (Phase III) at 12 GPa, and finally to a substitutional alloy (Phase IV, *I*-3*m*) at 14 GPa. Four superconducting phases were identified via temperature-dependent resistivity measurements under high pressure. Topological superconductivity can be realized in the first superconducting phase due to proximity effect between superconducting bulk states and Dirac type surface states [9]. However, the crystal structure at high pressure and low temperature remains intact. Since the superconducting critical pressure is very close to the phase transition pressure at room temperature, it is still a doubt whether the superconducting phase transition is related to the structural phase transition [21].

In this paper we addressed the high pressure low temperature angle-dispersive powder X-ray diffraction (ADXRD). No phase transition was detected up to 10 GPa at 8 K. Phase transition from Phase I to Phase II was observed between 8 K and 45 K at 8 GPa. In contrast to the previous reports, we discussed the superconducting and topological properties of p-type Bi_2Te_3 under high pressure and low temperature.

2. Experiments

Bi_2Te_3 crystals were grown using Bridgeman method. High purity Bi (99.999%) and Te (99.999%) with stoichiometric ratio were mixed, ground to fine powder and then pressed into pellets. The pellets were loaded into a quartz ampoule and sealed in vacuum. The ampoule was put into muffle furnace, heated to 1000 °C and kept for 3 days. After that, the furnace slowly cooled with the rate of 5 °C/hour to 500 °C, followed by furnace cooling. The final product can be easily cleaved into thin small sheets.

The final product was identified by X-ray powder diffraction (XRD). The XRD data was taken by a Phillips X′PERT using Cu Kα radiation. Fine powder was ground from cleaved specimen. *In situ* high pressure low temperature ADXRD experiments with synchrotron radiation were performed at HPCAT (Beam line 16BM-D and 16ID-B) of Advanced Photon Source using a Mao-Bell diamond anvil cell (DAC). We carried

* Corresponding author at: Faculty of Electrical Engineering and Computer Science, Ningbo University, Ningbo 315211, China.
** Corresponding author.
E-mail addresses: zhangjunliang@nbu.edu.cn (J.L. Zhang), Jin@iphy.ac.cn (C.Q. Jin).

http://dx.doi.org/10.1016/j.physb.2017.06.042
Received 11 April 2017; Received in revised form 11 June 2017; Accepted 12 June 2017
Available online 16 June 2017
0921-4526/ © 2017 Elsevier B.V. All rights reserved.

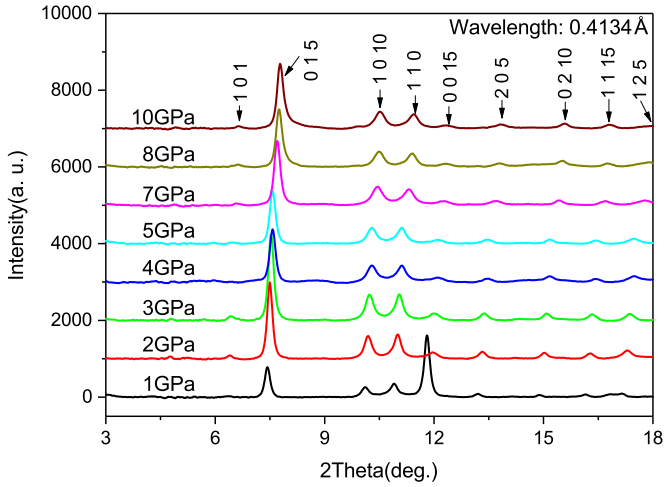

Fig. 1. ADXRD patterns of Bi_2Te_3 under various pressure points at 8 K.

out two independent ADXRD measurements. One measurement was carried out at 8 K under various pressure and the other was under 8 GPa at various temperature from 8 K to 260 K. The wavelength in the two measurements is 0.4134 Å and 0.3982 Å respectively. Helium was loaded into the sample chamber as pressure transmitting medium to guarantee hydrostatic condition. Pressure was calibrated using ruby fluorescence scale with a tiny ruby in sample chamber [22]. The Debye rings were recorded with image plate. ADXRD patterns were integrated from the images using FIT2d software [23].

3. Results

Fig. 1 shows in situ ADXRD pattern of Bi_2Te_3 at 8 K under various pressures up to 10 GPa. The peaks in ADXRD pattern under 1 GPa can be indexed with Phase I structure. The difference in peak intensity between 1 GPa and ambient pressure is caused by the crystal orientation under pressure. Peaks shift to the larger angle with increasing pressure due to the reduction of crystal lattice. No new peak appears in the pattern, indicating that Phase I persists up to 10 GPa at 8 K.

Temperature-dependent ADXRD patterns under 8 GPa are shown in Fig. 2. All peaks of ADXRD pattern at 8 K can be indexed with Phase I, which is consistent with the above experimental results. A new set of diffraction peaks appear in the pattern of 45 K, indicating that a phase transition occurs between 8 K and 45 K. The pattern remains essentially unchanged from 45 K to room temperature.

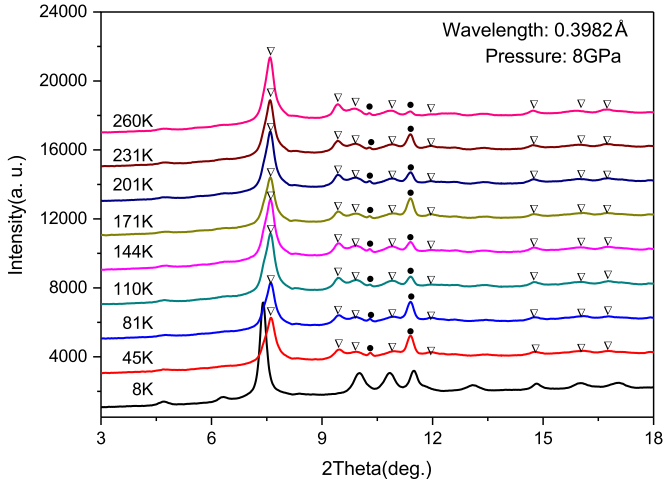

Fig. 2. ADXRD patterns of Bi_2Te_3 under 8 GPa under various temperatures. ▽ indicates the diffraction peaks belong to Phase II. • indicates the diffraction peaks of gasket.

4. Discussion

According to the ADXRD results, no structure phase transition occurs at 8 K under high pressure up to 10 GPa. Structure phase transition occurs between 8 K and 45 K under 8 GPa. In order to study the new structure after phase transition, we carefully compared the ADXRD patterns at 45 K and higher temperatures with those of high pressure phases reported previously [9,14,16,18]. The d-spacings and normalized intensities corresponding to the new diffraction peaks are very close to those of Phase II, indicating that the new peaks are from Phase II. The isotherm process at 8 K from 8 GPa to 10 GPa actually was realized by being heated from 8 K to 50 K at 8 GPa, then pressurized to 10 GPa and cooled to 8 K. Bi_2Te_3 undergoes a phase transition from Phase I to Phase II during heated to 50 K at 8 GPa, maintains Phase II during pressurization from 8 GPa to 10 GPa at 50 K. As Bi_2Te_3 is in Phase I at 8 K and 10 GPa, it undergoes a phase transition from Phase II back to Phase I during the cooling process from 50 K to 8 K under 10 GPa. As Phase I is more stable at 8 GPa than at 10 GPa, we believe that the phase transition from Phase I to Phase II is reversible.

ADXRD patterns in Fig. 1 were refined using EXPGUI GSAS program package with Rietveld method [24]. Fig. 3 shows the refined results of ADXRD patterns at 2 GPa and 8 GPa. Lattice parameters of unit cell and atomic coordinates are listed in Table 1. The refined lattice parameters and volumes at various pressures are plotted in Fig. 4. The pressure dependence of volume are fitted by using the Birch–Murnaghan (B–M) equation

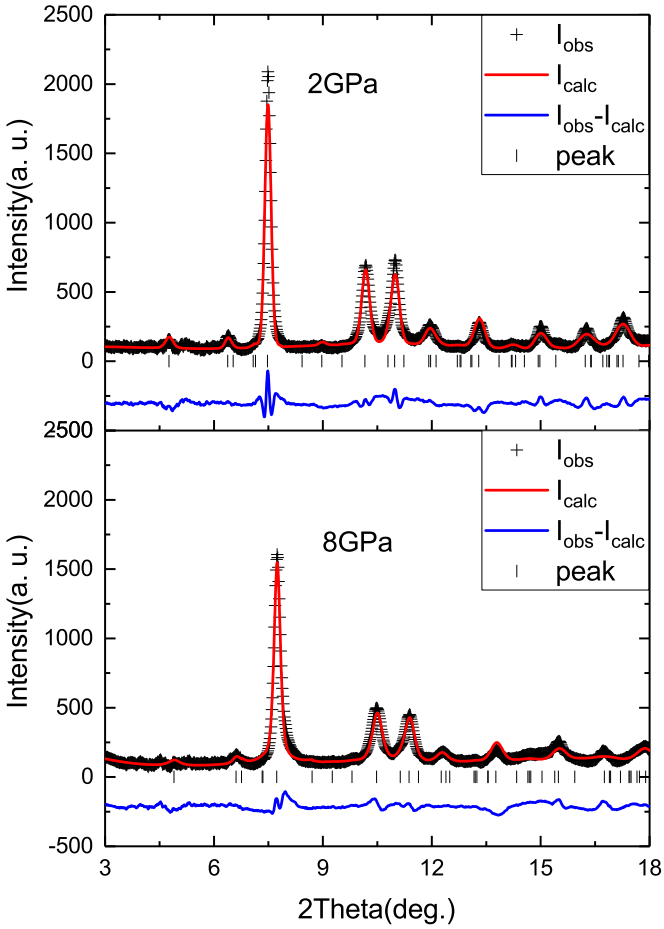

Fig. 3. Rietveld refinement results of Bi_2Te_3 under 2 GPa and 8 GPa. The + symbols and red lines represent the observed data and Rietveld fits respectively. The blue lines represent the difference of intensity between the observed data and the fitted data. The XRD peaks are indicated by vertical bars. (For interpretation of the references to color in this figure legend, the reader is referred to the web version of this article.)

Table 1
Lattice parameters and atomic coordinates under pressure, derived from Rietveld refinements.

Pressure	Lattice parameters	Atomic coordinates			
(GPa)	(Å)	(fractional)			
		Atom	x	y	z
1 GPa	a =b = 4.3674	Bi1(6c)	0	0	0.4000
	c = 30.0228	Te1(3a)	0	0	0
		Te2(6c)	0	0	0.2070
2 GPa	a = b = 4.3227	Bi1(6c)	0	0	0.3999
	c = 29.8708	Te1(3a)	0	0	0
		Te2(6c)	0	0	0.2077
3 GPa	a =b = 4.3054	Bi1(6c)	0	0	0.4002
	c = 29.7343	Te1(3a)	0	0	0
		Te2(6c)	0	0	0.2069
4 GPa	a = b = 4.2807	Bi1(6c)	0	0	0.3995
	c = 29.5325	Te1(3a)	0	0	0
		Te2(6c)	0	0	0.2038
5 GPa	a =b = 4.2509	Bi1(6c)	0	0	0.4002
	c = 29.3518	Te1(3a)	0	0	0
		Te2(6c)	0	0	0.2061
7 GPa	a = b = 4.2043	Bi1(6c)	0	0	0.4030
	c = 29.1570	Te1(3a)	0	0	0
		Te2(6c)	0	0	0.2040
8 GPa	a = b = 4.1723	Bi1(6c)	0	0	0.4040
	c = 29.0328	Te1(3a)	0	0	0
		Te2(6c)	0	0	0.2032
10 GPa	a = b = 4.1545	Bi1(6c)	0	0	0.4040
	c = 28.9628	Te1(3a)	0	0	0
		Te2(6c)	0	0	0.2032

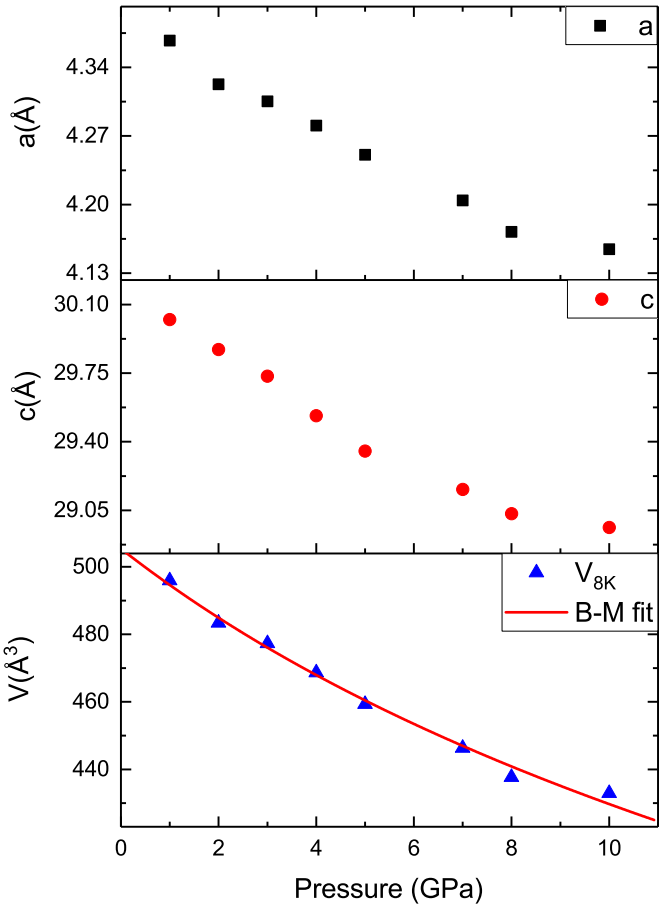

Fig. 4. Pressure dependence of lattice parameters and unit cell volume of Bi_2Te_3 at 8 K. The red line is the fitting result of B-M equation. (For interpretation of the references to color in this figure legend, the reader is referred to the web version of this article.)

$$p = \frac{3}{2}B_0\left[\left(\frac{V}{V_0}\right)^{-\frac{7}{3}} - \left(\frac{V}{V_0}\right)^{-\frac{5}{3}}\right]\left\{1 - \left(3 - \frac{3}{4}B_0'\right)\left[\left(\frac{V}{V_0}\right)^{-\frac{2}{3}} - 1\right]\right\},$$

where V_0 is the zero-pressure volume, B_0 is the bulk modulus at ambient pressure, and B_0' is the derivative of the bulk modulus with respect to pressure. Assuming B_0' = 4, the ambient pressure bulk modulus B_0 is 45 ± 3 GPa. The fitted result is shown with red line in Fig. 4.

Now we turn to the superconductivity of p-type Bi_2Te_3 under high pressure. The onset of superconductivity appears at ~ 3 GPa in DAC with solid-state pressure media [9,18,25]. However superconductivity appears above ~ 7 GPa under hydrostatic condition [21]. As the superconducting T_c is below 8 K, we speculate that the superconductivity below 10 GPa is related to *R*-3*m* phase. The superconducting phase below 7 GPa is due to the uniaxial strain effect in the *R*-3*m* phase. The hole-like carriers in normal states [9,18,25] indicate that the non-zero bulk energy gap existed. It is theoretically predicted that topological surface states of Phase I remains stable under pressure [9]. For the bulk superconducting phase at 7 GPa, topological superconductivity might be realized on the interface states due to proximity effect with the bulk superconducting states.

5. Conclusions

In conclusion, structural stability and phase transition of Bi_2Te_3 have been investigated through high-pressure low-temperature ADXRD up to 10 GPa. Phase I is stable at 8 K up to 10 GPa. Under 8 GPa, a phase transition from Phase I to Phase II was observed between 8 K and 45 K. ADXRD patterns collected at 8 K were refined. The pressure-dependent volume relationship was fitted by the Birch–Murnaghan (B–M) equation. The ambient pressure bulk modulus B_0 is 45 ± 3 GPa. The superconductivity below 10 GPa is related to Phase I. Topological superconductivity might be realized at the interface states.

Acknowledgments

The work is supported by National Natural Science Foundation of China (Grant No. 11504189), Zhejiang Provincial Natural Science Foundation of China (Grant No. LY16A040001), the Scientific Research Fund of Zhejiang Provincial Education Department (Grant No. Y201533846), and K.C. Wong Magna Fund in Ningbo University.

References

[1] S. Murakami, N. Nagaosa, S.C. Zhang, Spin-Hall insulator, Phys. Rev. Lett. 93 (2004) 156804.
[2] C.L. Kane, E.J. Mele, Z(2) topological order and the quantum spin Hall effect, Phys. Rev. Lett. 95 (2005) 146802.
[3] B.A. Bernevig, T.L. Hughes, S.C. Zhang, Quantum spin Hall effect and topological phase transition in HgTe quantum wells, Science 314 (2006) 1757–1761.
[4] D. Hsieh, et al., A topological Dirac insulator in a quantum spin Hall phase, Nature 452 (2008) (970-U5).
[5] H.J. Zhang, et al., Topological insulators in Bi2Se3, Bi2Te3 and Sb2Te3 with a single Dirac cone on the surface, Nat. Phys. 5 (2009) 438–442.
[6] Y.L. Chen, et al., Experimental realization of a three-dimensional topological insulator, Bi2Te3, Science 325 (2009) 178–181.
[7] L. Fu, C.L. Kane, Superconducting proximity effect and Majorana fermions at the surface of a topological insulator, Phys. Rev. Lett. 100 (2008) 096407.
[8] Y.S. Hor, et al., Superconductivity and non-metallicity induced by doping the topological insulators Bi2Se3 and Bi2Te3, J. Phys. Chem. Solids 72 (2011) 572.
[9] J.L. Zhang, et al., Pressure-induced superconductivity in topological parent compound Bi2Te3, Proc. Natl. Acad. Sci. USA 108 (2011) 24–28.
[10] J. Zhu, et al., Superconductivity in topological insulator Sb2Te3 induced by pressure, Sci. Rep. 3 (2013). http://dx.doi.org/10.1038/srep02016.
[11] M.Z. Hasan, C.L. Kane, Colloquium: topological insulators, Rev. Mod. Phys. 82 (2010) 3045.
[12] X.L. Qi, S.-C. Zhang, Topological insulators and superconductors, Rev. Mod. Phys. 83 (2011) 1057.
[13] X.L. Qi, et al., Time-reversal-invariant topological superconductors and superfluids in two and three dimensions, Phys. Rev. Lett. 102 (2009) 187001.
[14] A. Nakayama, et al., Structural phase transition in Bi2Te3 under high pressure,

High Press. Res. 29 (2009) 245–249.
[15] M. Einaga, et al., Pressure-induced phase transition of Bi2Te3 to a bcc structure, Phys. Rev. B 83 (2011) 092102.
[16] L. Zhu, et al., Substitutional alloy of Bi and Te at high pressure, Phys. Rev. Lett. 106 (2011) 145501.
[17] G.K. Pradhan, et al., Raman signatures of pressure induced electronic topological and structural transitions in Bi2Te3, Solid State Commun. 152 (2012) 284–287.
[18] S.J. Zhang, et al., The comprehensive phase evolution for Bi2Te3 topological compound as function of pressure, J. Appl. Phys. 111 (2012) 112630.
[19] I. Loa, et al., Atomic ordering in cubic bismuth telluride alloy phases at high pressure, Phys. Rev. B 93 (2016) 224109.
[20] K. Zhao, et al., Pressure-induced anomalies in structure, charge density and transport properties of Bi2Te3: a first principles study, J. Alloy. Compd. 661 (2016) 428–434.
[21] K. Matsubayashi, et al., Superconductivity in the topological insulator Bi2Te3 under hydrostatic pressure, Phys. Rev. B 90 (2014) 125126.
[22] H.K. Mao, J. Xu, P.M. Bell, Calibration of the ruby pressure gauge to 800 kbar under quasi-hydrostatic conditions, J. Geophys. Res. 91 (1986) 4673.
[23] A.P. Hammersley, et al., Two-dimensional detector software: from real detector to idealised image or two-theta scan, High Press. Res. 14 (1996) 235–248.
[24] B.H. Toby, EXPGUI, a graphical user interface for GSAS, J. Appl. Crystallogr. 34 (2001) 210–213.
[25] C. Zhang, et al., Phase diagram of a pressure-induced superconducting state and its relation to the Hall coefficient of Bi2Te3 single crystals, Phys. Rev. B 83 (2011) 140504.